MICROSTRUCTURE OF THIN-GAUGE AUSTENITIC AND FERRITIC STAINLESS STEEL JOINTS BRAZED USING METGLAS® AMORPHOUS FOIL

E.A. Leone[1], A. Rabinkin[2], B. Sarna[3]
[1] Honeywell (USA), [2] Metglas Inc. (USA), [3] DCL (Canada)
[2] E-mail: anatol.rabinkin@metglas.com

ABSTRACT

Vastly different microstructures are formed in 304LN austenitic and Fecralloy® ferritic stainless steel joints brazed with Ni-15Cr-1.4B-7.25Si (MBF-51) and Ni-19Cr-1.5B-7.3Si (MBF-50), filler metals, respectively. These joints were cut from an industrial heat exchanger and a metallic catalyst support that were subjected to a short optimal brazing cycle in a vacuum furnace. A detailed description is given of the composition and morphology of phases evolved in these brazements, as a result of complex metallurgical reactions between the base and filler metals. A new metallurgical reaction was discovered between Fe-20Cr-5Al Fecralloy base metal (BM) having b.c.c. crystal lattice, and the Ni and B from MBF-50 (Ni-19Cr-1.5B-7.25Si) brazing filler metal (FM). This reaction resulted in the precipitation of fine, regularly distributed Ni_x $(Al)_y$ particles in the base metal matrix phase, thus strengthening Fecralloy brazements. The microstructure discovered in this work is remarkably similar to that of conventional precipitation-hardened, heat resistant alloys. Therefore, these joints can withstand years of service in the brutal environment observed in automotive exhaust pipes.

IIW-Thesaurus keywords: *Austenitic stainless steels; Stainless steels; Steels; Ferritic stainless steels; Microstructure; Brazed joints; Amorphous metals; Parent material; Brazing fillers; Filler materials; Gap; Joint preparation; Age hardening; Hardening; Heat treatment; Reference lists.*

1 INTRODUCTION

Advanced brazed thin-walled structures and honeycombs have been increasingly used in modern manufacturing. Compact plate-plate and plate-fin heat exchangers, exhaust gas catalytic converters for cars and trucks, fuel converters for fuel cells, seals for aircraft turbines are only a few examples where these brazed assemblies play a critical role in achieving superior energy savings and environmental protection. Other advantages include very low weight combined with high strength per unit weight, compactness, a one-step economical fabrication cycle and relatively low production costs.

In most, if not in all their applications, the base metals (BM)s of the aforementioned brazed structures are made of stainless steels, superalloys, and powder metallurgy foils having thicknesses in order of a few mils (50-200 μm). In spite of such minute thickness, these structures withstand a high temperature/oxidation environment for a very long time without noticeable deterioration. The filler metals (FM)s used are Ni/Co-based alloys that are covered by AWS A.5 specifications as the BNi- and BCo- classifications. These classifications can be applied in forms of powders, powder-based pastes or tapes, or Metglas® amorphous brazing foils (designated MBF). The latter have been used predominantly due to their minute 25-50 μm (1.0-2.0 mil) thickness, resulting in a much lower BM erosion when compared to the powder forms. The low erosion rate is an extremely critical factor for thin-walled parts. Inherently flexible amorphous foils are also convenient to handle when automatically assembling many precise parts in one unit prior to brazing operations. Earlier, the optimization of brazing processing of plate/plate and plate/fin stainless steel parts was reported and some data on their microstructure and properties were presented [1-4]. The combinations of BM/FM studied previously were as follows: 316L/MBF-51/316L [1, 3], 430/MBF-20/430 [2, 3], 436/MBF-20/436 [4], and PM2000/MBF-50, -51/PM2000 [2, 3].

This work describes results of detailed microstructural studies of joints manufactured of 304LN and Fecralloy materials as BMs and MBF-51 and MBF-50 as FMs, correspondingly. Table 1 presents their complete chemical compositions (wt. %). Such combinations have a wide range of industrial applications but have never been analysed before. The joints selected for analysis were taken from some industrial heat exchanger (HE) and a metal catalytic support (MCS). In addition, the first example presents a series of joints with BM parts having different thickness; whereas all the other processing parameters were the same. Therefore, the effect of thickness

Doc. IIW-1713-05 (ex-doc. I-1147-04) recommended for publication by Commission I “Brazing, soldering, thermal cutting, and flame processes”.

Table 1 – Composition, thickness of the base and filler metals, and brazing conditions

Alloy	Composition	Part thickness (μm)	Brazing conditions in vacuum (T, t)
Austenitic BM			
BM -304LN	Fe-10Ni-19Cr-2Mn-1Si-0.1N	Core plates – 305 Fins – 101	1 172 °C /10 min
FM-MBF-51	Ni-15Cr-1.4B-7.25Si	37	
Ferritic BM			
BM -Fecralloy	Fe-20Cr-5Al-R.E. oxides –	Corrugated fin – 50 Smooth fin – 50	1 172 °C /10 min
FM-MBF-50	Ni-15Cr-1.4B-7.25Si	25	

differences on joint microstructure could be assessed. Secondly, the Fecralloy/MBF-50 combination provides information on the structure of joints in metal catalytic supports for automotive exhaust systems. Such systems must withstand very challenging service environment without deterioration of the braze joints for many years.

2 BRAZED SAMPLES AND MICROSTRUCTURAL ANALYTICAL METHODS

Figures 1 a)-d) show cross-sectional views of four typical types of joints that were used to completely fuse all parts comprising a plate/fin HE. The brazements separate and seal two sets of mutually adjacent and parallel, but isolated channels, which share the same enclosing surfaces. Each system of channels carries either a cold or a hot medium. A good thermal contact through thin channels walls between the media provides efficient energy transfer. Two types of thin fin/plate joints are shown in Figures 1 a) and 1 b), and two types of thick plate/plate joints are shown in Figures 1 c) and 1 d).

The above HE parts had the following thicknesses:
– core plates: 0.305 mm (12 mil);
– fins: 0.101 mm (4 mil).

MBF-51 amorphous alloy in the foil form having a thickness of 37 μm (1.5 mil) was used as a brazing FM. It is worth noting that preplaced preforms of MBF-51 foils covered the entire part cross-sections in each alternating fin/plate and plate/plate, sequence. Therefore, the preform had a much larger surface than that of all joints located in each individual cross-section. The excessive amount of MBF-51 metal relative to the joint cross-sections was able to completely fill all potential variations and irregularities in gap dimensions by the strong capillary effects. This results in the formation of well-shaped fillets. The same situation with respect to the ratio of the preform and BM surfaces existed in the second application (i.e. the MCS) presented below.

The following HE brazing cycle under vacuum was used in 304LN/MBF-51 case:
– Heating to 1 038 °C (1 900 °F) at 28 °C/min (50 °F/min) and holding for 15 minutes;
– Heating to 1 172 °C (2 140 °F) at 33 °C (60 °F/min) and holding for 10 minutes;
– Cooling in vacuum to 1 038 °C (1 900 °F) followed by forced nitrogen cooling to < 66 °C (150 °F).

The choice of a short brazing holding time segment was correct in this case because it yielded minimal erosion. However, such heat treating conditions would not be easy to reproduce when manufacturing large industrial batches of HE in industrial furnaces, since the batches have a substantial weight. Unfortunately, this results in unavoidable thermal inertia and low maximum heating rate of parts.

The HE under this study was visually examined at about 10-20 times magnification before cutting samples for the metallographic analysis. It was found that all joints had good-shaped fillets with well advanced “beach lines” observed on the part surfaces.

The MCS sample used in this study was made of Fecralloy® 50 μm thick corrugated/ flat foils produced by Sandvik and MBF-50 25 μm thick foil, used as the BM and FM, correspondingly. The general view of a cross-section is shown in Figures 1 e) and 1 f). This sample was made in accordance with materials and dimensions of the core of a standard metallic catalyst support used in automotive exhaust pipes. It was manufactured using the following braze cycle in a vacuum of about 1.33×10^{-5} Pa (1×10^{-5} torr):
– Heating to 950 °C and holding for 15 min ;
– Heating to 1 175 °C and holding for 15 min ;
– Cooling in furnace under vacuum to 200 °C with the power off ;
– Final cooling to 25 °C in a nitrogen atmosphere.

Samples for metallography were removed from both parts by cutting across the structure with a diamond wheel, embedding the pieces in epoxy, and polishing down to a 1-μm diamond finish. The samples were then coated with a thin carbon film to avoid charging during SEM and EDX analysis. The microstructure of all typical joints present in the cross-sections were subjected to backscattered electron imaging (BEI) and energy dispersive x-ray analysis (EDXA) using a JEOL 840 SEM, equipped with an EVEX-QDD quantum dot x-ray detector. X-ray spectra and maps were made only for elemental Fe, Ni, Cr, and Si. In this investigation, boron could not be easily identified. However, it is assumed that any phase observed which appears “dark” and yields only characteristic chromium x-ray lines are considered to be chromium borides. It is well known that dark BEI contrasting phases are associated with low atomic number (light) elements. In previous studies of

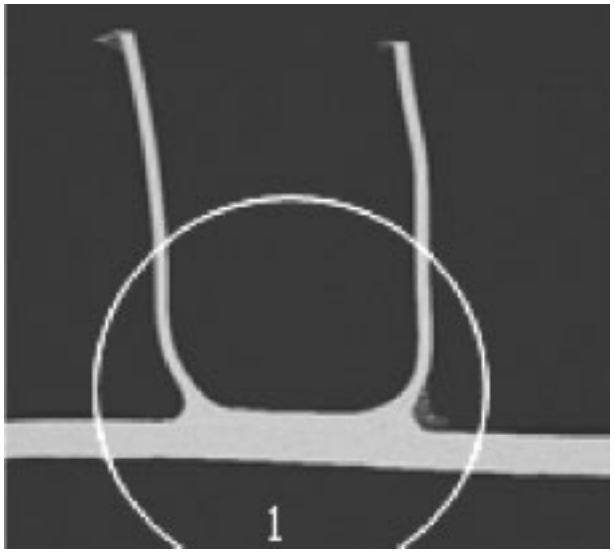

a) Joints made of 304LN stainless steel and brazed with MBF-51 foil

b) Joints made of 304LN stainless steel and brazed with MBF-51 foil

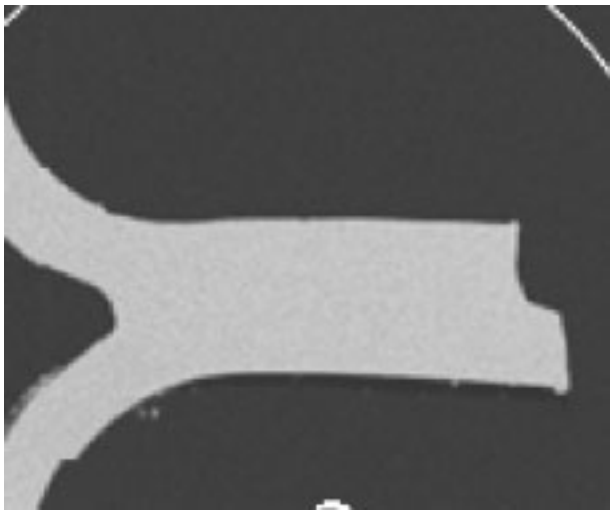

c) Joints made of 304LN stainless steel and brazed with MBF-51 foil

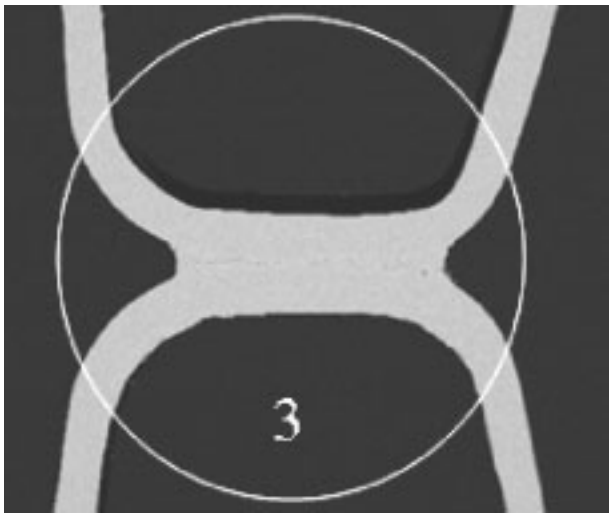

d) Joints made of 304LN stainless steel and brazed with MBF-51 foil

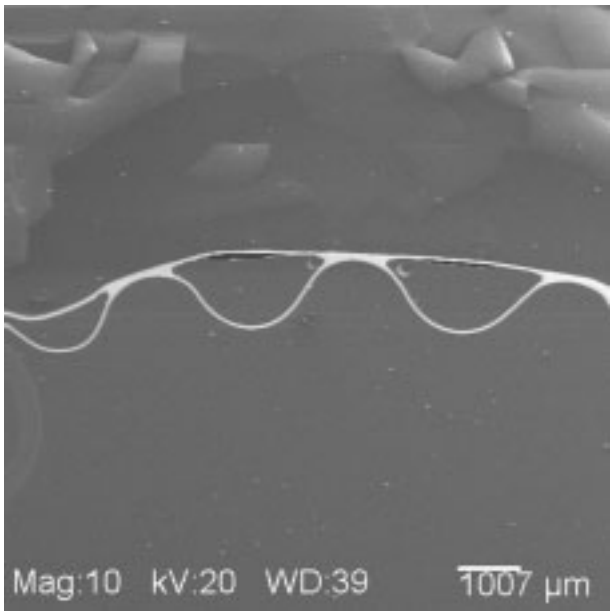

e) Joints made of Fecralloy® MCS brazed with MBF-50

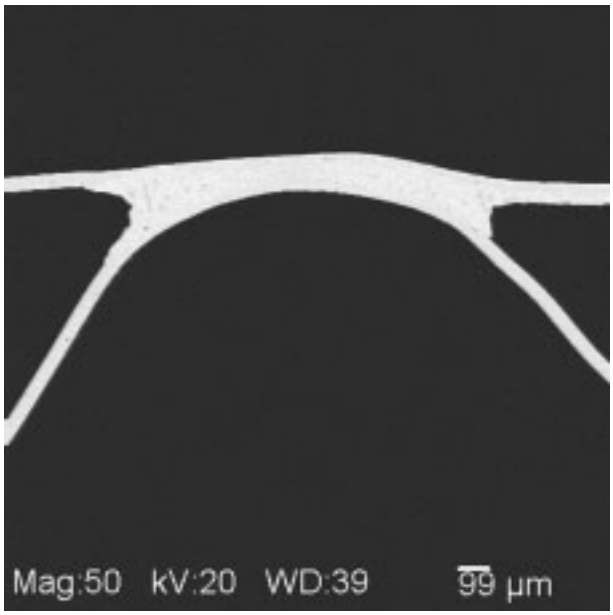

f) Joints made of Fecralloy® MCS brazed with MBF-50

Figure 1 – General views of the elemental joints of the heat exchanger cross-section

other stainless steel/MBF joints, scanning Auger microscopy (SAM) was used to characterise these dark contrasting phases. Auger analysis is capable of identifying boron and carbon directly, proving unequivocally that boron was present in the phases with such BEI SEM appearance [5].

3 RESULTS

3.1 304LN stainless steel joints brazed with MBF-51 brazing FM

3.1.1 Fin/plate joints

As can be seen in Figures 1 and 2, good fillets are formed upon brazing demonstrating excellent wetting and low contact angle ($\theta \rightarrow 0^{o}$). Importantly, no open porosity was observed at the fillet surface and only a couple of pores were found in one of the fillets. All internal joint regions were free from porosity.

Typical of most brazements, the entire analysed structure can be divided morphologically into four segments:

(1) the major central joint segment with a more or less even and minute thickness;

(2) the BM areas adjoining the interface;

(3) the remainder of BM unaffected by brazing; and

(4) the fillets, with much larger thickness that increases outwardly in both directions from the centre of the joint.

Measurements showed that the degree of BM erosion was not very large. Its magnitude varied from 5-10 μm in the central segment of the joint and up to 10-20 μm in the areas adjoining the fillets. The latter had a much larger liquid FM volume relative to the surface area of contacting BM than that in the major joint section. Therefore, the fillets had dissolved a larger amount of the BM without even being saturated. They also contained larger fractions of the initial amounts of boron and silicon.

The only phases observed in the longest internal joint regions, including the interface zone, are the (Ni, Cr, Si, Fe) solid solution matrix phase and $Cr_x B_y$ borides, as seen in Figure 2. The latter segregated mostly within the BM area adjoining the interface. The joint matrix phase had an even distribution of Ni, Si, and Cr. The iron distribution decreased smoothly from the BM/ joint interface to the middle of the joint. These conclusions were drawn from data obtained from scanned and measured elemental concentration profiles in various locations across the joint. Examples of such profiles are given in Figure 3. Interestingly, no separate nickel silicide particles were observed in either the central joint segment or the BM. The same phases were also observed in previous work in which 316L SS/MBF-51 joints were studied [1]. Data on composition of the central part of the joint are given in the Table in Figure 3. These data show the presence of Si, Ni, Cr, and Fe in the matrix phase. The chromium concentration is slightly higher than that initially observed in the virgin MBF-51 ribbon; 16.7 vs. 15 wt. %. It is very probable that chromium diffused from the BM where its concentration was higher. The silicon concentration in the Table is too high to be accepted as reliable, i.e., 11.5 vs. 7.25 wt. % in the virgin MBF-51 ribbon. No attempt was made to verify this data.

The joint interface very sharply separates the areas formed by the FM crystallization and the bulk of the BM (Figure 4). The microstructure of the BM parts is not too different across the joint circumference even in proximity of the fillet. It consists of three consecutive morpho-

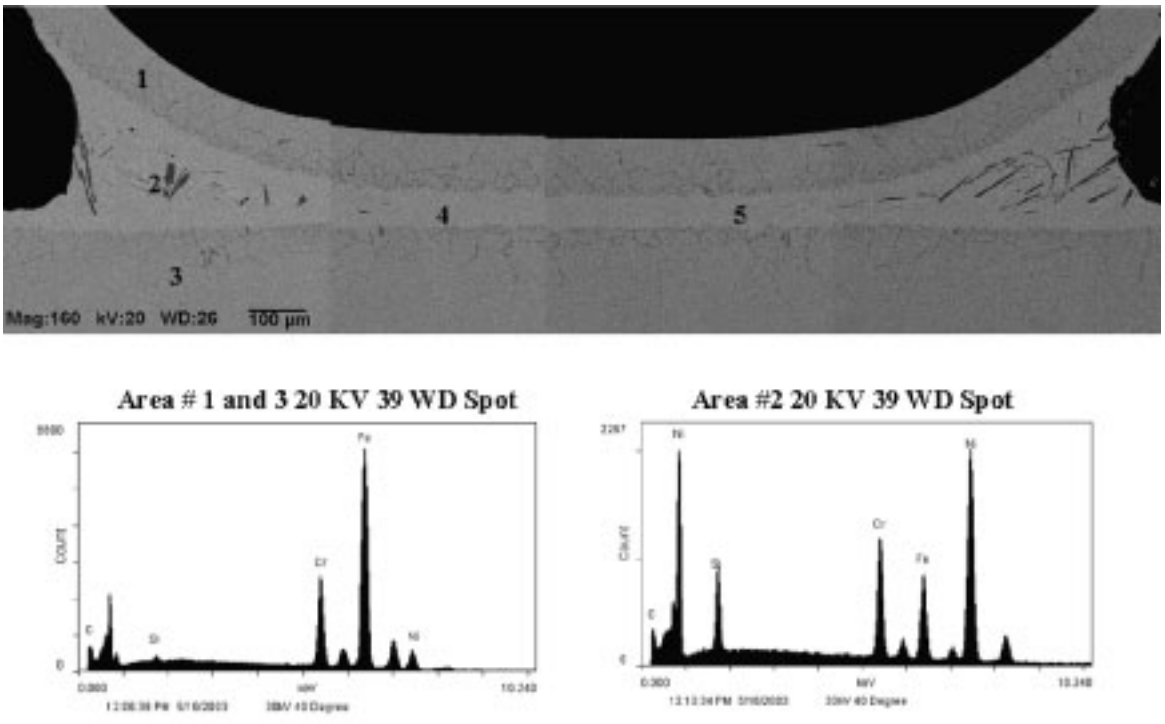

Figure 2 – Total view of the U-shaped fin and plate microstructure and energy dispersive x-ray spectra taken from the spots marked by corresponding numbers

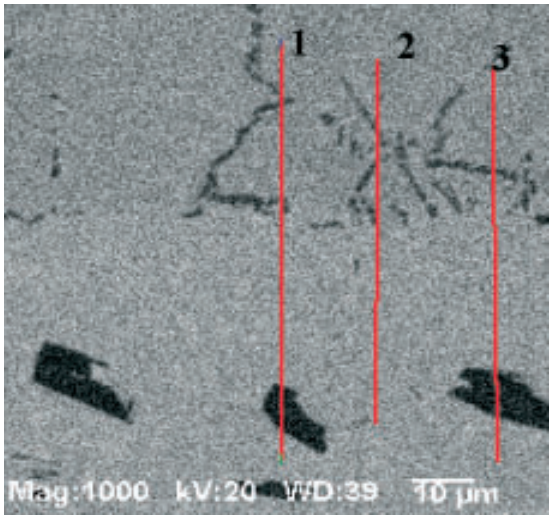

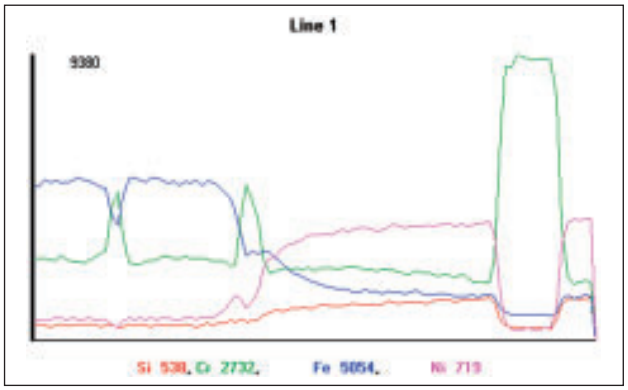

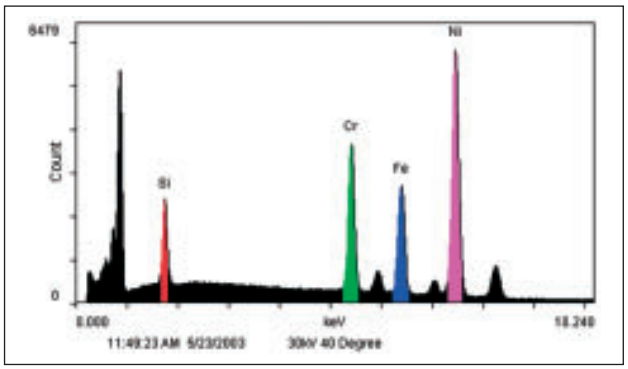

Composition of the braze solid solution matrix phase calculated using x-ray spectrum data

Elem	AT %	WT %	KA	KF	KZ	Int	P/bkg
Si K	20.8	11.5	0.277	1.001	1.078	155.0	3.1
Cr K	16.3	16.7	0.965	1.119	0.972	389.1	10.1
Fe K	14.7	16.1	0.933	1.139	0.976	319.3	8.7
Ni K	48.2	55.7	0.923	1.000	0.996	741.7	26.1

Figure 3 – Elemental distribution across the interface of a fin/plate sample in the fillet vicinity

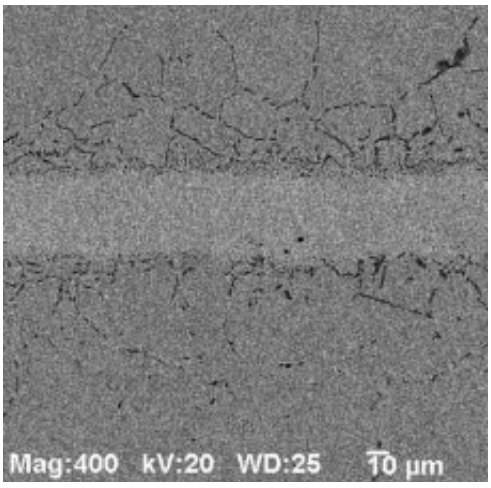

a) General appearance

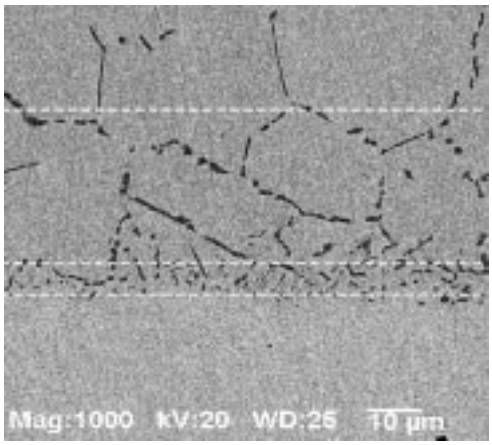

b) The interface area under high magnifications
(two types of the BM grains are clearly seen)

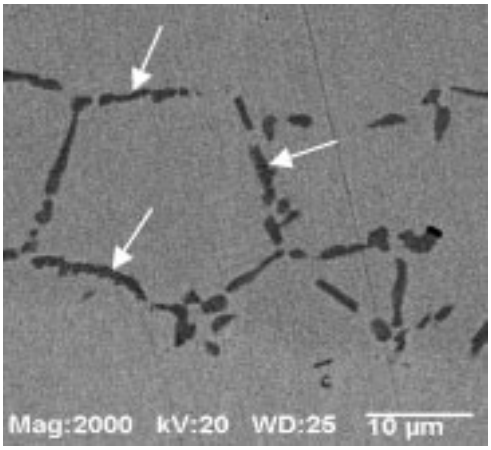

c) The interface area under high magnifications
(two types of the BM grains are clearly seen)

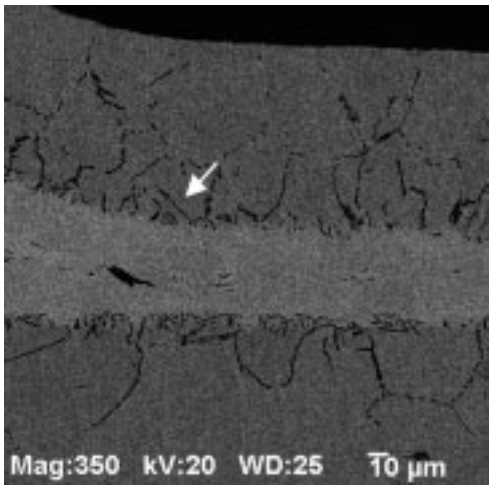

d) Chromium boride segregations at twin boundaries (arrow)

Figure 4 – Fin/plate joint microstructure

logical zones [Figure 4 b)]. The first 5 to 8 μm-wide zone, adjoining the joint interface contains fine, narrow chromium boride platelets formed within the original grains [Figure 4 b)]. This zone has the appearance of the perlite structure in carbon steels. The second 50 to 80 μm-wide zone contains chromium borides segregated as separate, narrow, island-like particles at the BM grain boundaries [Figure 4 c), arrows)]. The amount of boron is substantial to segregate even at twin boundaries [Figure 4 d), arrows] but no segregation in the bulk of the grains is observed. This pattern is similar to that in many other cases in which stainless steels were brazed with MBFs containing boron [1]. It happens because boron has an extremely low boron intergranular solubility in all highly alloyed materials. This is caused by a large misfit of its atomic size with sizes of both interstitial and substitutional sites in alloys crystal lattices [3, 5].

In the second zone, close to the interface, the borides formed complete shells covering the most of the grain boundary surfaces [Figure 4 c)]. Because boride segregation in 300-series stainless steels occurs only at the grain and the twin boundaries [1, 5], their width does not exceed 2-3 μm. Further from the interface, the borides segregated only at some parts of the grain surface [Figure 4 a)]. Starting at about 80 μm distance, they are not observed at all. Therefore, from the third zone outward, the BM is unaffected by interaction with the FM.

The low sensitivity of the BM microstructure to the joint thickness is due to the specifics of diffusion processes during a rather short time of the brazing cycle. In the beginning of the metallurgical interaction between the liquid FM and the solid BM, substantial gradients of elemental concentrations across the interface were created for boron, silicon, iron, and nickel. The difference in the chromium concentrations in both interacting alloys is not very large. At the same time, the activity of boron in the FM is lower due to effect of the silicon. Therefore, boron has a high driving force to diffuse into the 304LN steel and form chromium borides at the grain boundaries. In addition, the rate of boron diffusion is two orders of magnitude higher relative to that of silicon, and particularly greater than nickel and iron [6]. The mutual diffusion mass-transfers of other elements are rather small. So, boron diffuses very fast and evenly across the interface into the solid stainless steel, lowering its concentration in the liquid FM and simultaneously forming chromium borides in 304LN.

The degree of the boron depletion is inversely proportional to the volume (thickness) of the liquid in the gap. The 15 min brazing time was not sufficient to substantially change the initial elemental redistribution of Ni, Cr, Fe, and Si in the 50 to 70 μm thick joint areas. Only boron diffused into the BM to a degree at which a single (Ni, Cr, Si, Fe) – solid solution phase, depleted in boron, was formed upon crystallization. It is evident that the joints are completely free from secondary segregated phases in area of the gaps where the width did not exceed 60 to 80 μ (Figure 2). The joints with a single-phase (Ni-Cr-Fe-Si) – solid solution microstructure possessed high strength and ductility as shown in reference [1].

In regions where the joint width exceeded 70 to 80 μm, the chromium borides segregated upon cooling within the liquid phase. They have elongated platelet-like forms characteristic of solidified eutectic mixtures in which one of the components is an intermetallic phase (Figure 5). The fillet areas with 200 to 250 μm width have a well-developed eutectic structure in which silicon and boron

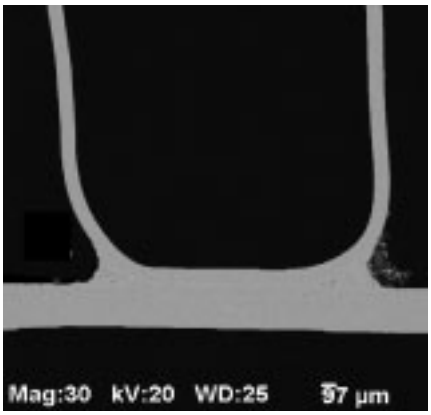

a)

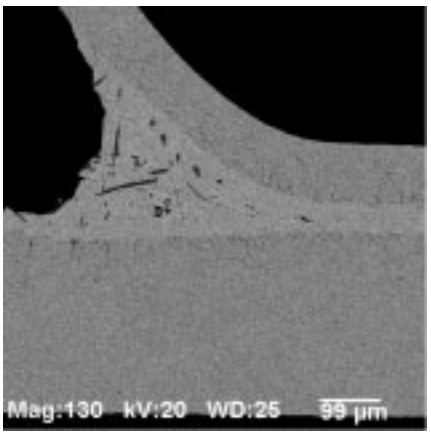

b)

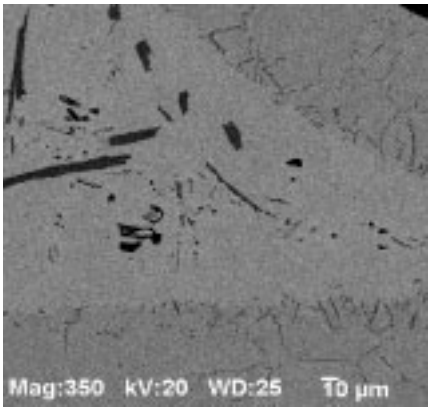

c)

Figure 5 – Fillets of a fin/plate 304LN joint

are both still present in large quantities [Figure 5 c)]. This eutectic consists of the (Ni, Cr, Si, Fe)-solid solution matrix phase, segregated chromium borides, and some regions enriched in silicon and nickel. They are intermixed with silicon-enriched regions. The total microstructure is similar to that of the core in cast ingots in which crystallization was accompanied by the liquation process.

The chromium borides, observed in fillets and in thicker (> 70 μm) external parts of the joints have various shapes [Figure 5 c)]. Some look like even-sized blocks, or elongated rectangular blocks. Others have a fan or feather-shaped morphology. They are intermixed mostly in thick fillet areas. The cross-sections of "blocky" particles sometimes reached 50 × 50 μm, whereas elongated needle-shaped particles were as long as 90 μm [Figures 2 and 5 c)].

According to [7], boron segregation at grain boundaries does not cause substantial embrittlement. On the other hand, large plate- and rod-like boride crystals present in fillets, particularly those piercing the fillet surfaces, may play a substantially negative role as potential sources of crack nucleation [1].

3.1.2 Plate/Plate joints

Figures 6 and 7 have high-magnification microstructural images of the joints shown in Figures 1 c) and 1 d). Here, the joints are enclosed between two 300 μm thick plates. The rounded shape of the plates, caused by the difficulties in pressing out completely flat surfaces in a very small area, yielded gaps with a variable width increasing in both directions from the central location. The microstructures shown in Figures 6 and 7 are very informative ones because they, again, clearly demon-

Note the appearance of eutectic microstructure in the joint areas thicker than 50-80 μm

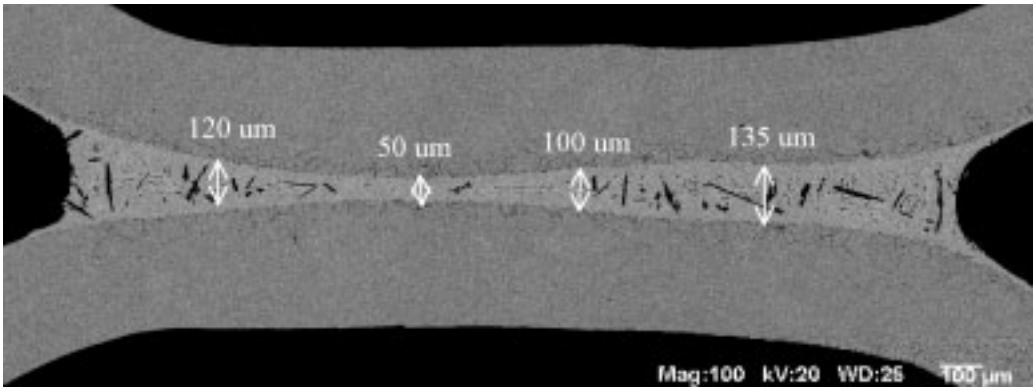

Figure 6 – Plate/plate 304LN/MBF-51/304LN joint

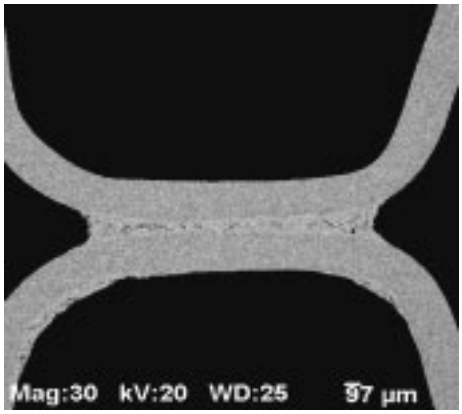

a) General view

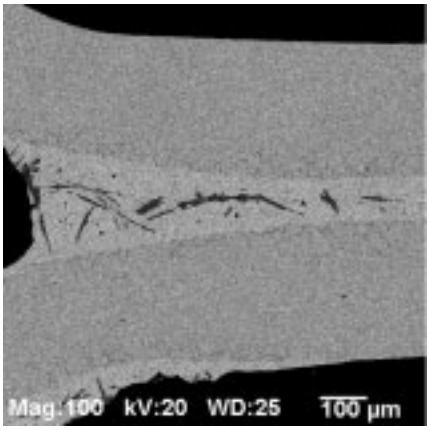

b) The fillet area

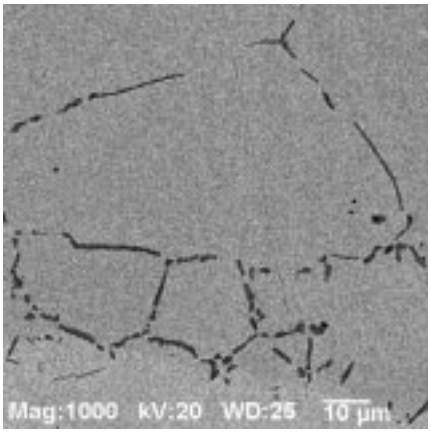

c) The base metal in the interface vicinity

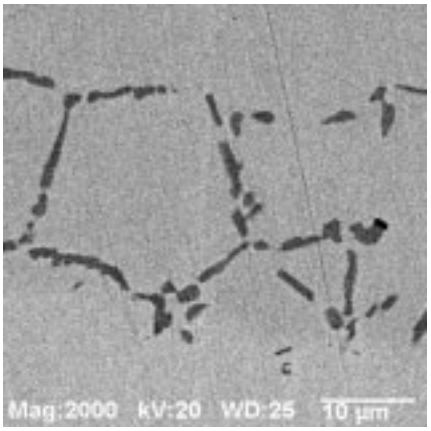

d) The base metal in the interface vicinity

Figure 7 – Different areas of the plate/plate joint

strate the sensitivity of the joint structure to the gap dimensions. These dimensions, in turn, determine the thickness of the liquid FM filling this gap due to capillary effects.

X-ray maps shown in Figure 8 demonstrate the elemental distribution of the joint. The general features of these joints, including fillets, are rather similar to the microstructure of the fin/plate joints. The BM microstructure looks like that of the plate in the previous case. One can see the same pattern of elemental distributions across the joins presented in the line-scans shown in Figure 9. One substantial different feature of the plate/plate joints structure vs. that of the fin/plates ones is the absence of small platelets in the interface zone. A couple of rows of small-sized BM grains are seen at the interface in some areas. Inversely, in other parts of the joints the BM grain dimension are unchanged and these grains directly contact the braze itself (Figure 9). The absence of many platelets of chromium borides in the interface area may be tentatively explained by a much larger BM volume. This led to a much larger boron concentration gradient in the BM interface area, resulting in a more intensive boron outflow into the BM, and smaller accumulations at the interface. Therefore, the boron concentration was insufficient to form the platelets. There was only enough boron present to decorate the grain boundaries, similar to the interface zone in the fin/plate case. Figure 6 demonstrates, again, the importance of limiting the joint thickness in order to avoid segregation of eutectic phases, thus producing a ductile single-phase joint.

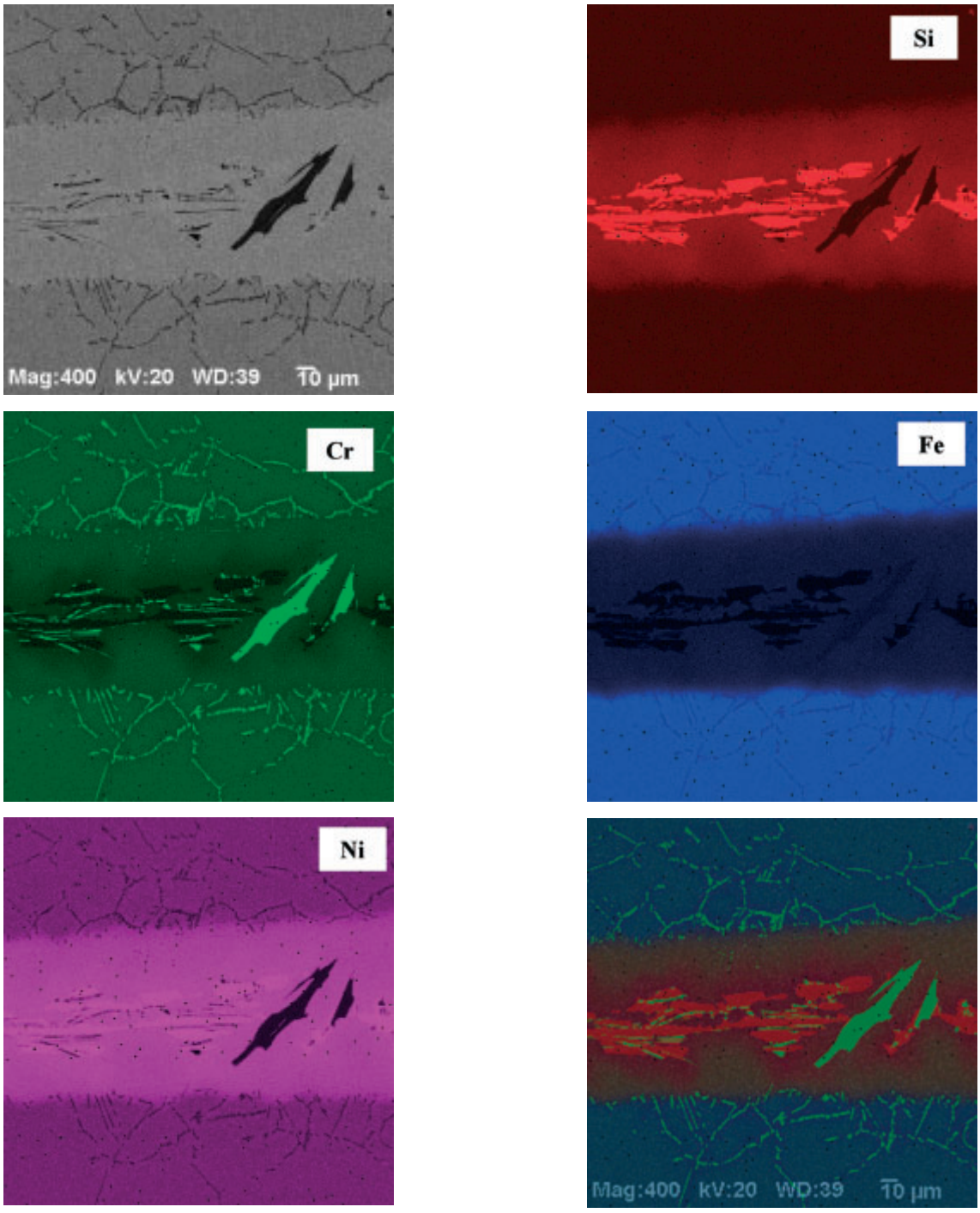

Figure 8 – Elemental distribution in the thick part of a plate/plate joint according to the x-ray mapping

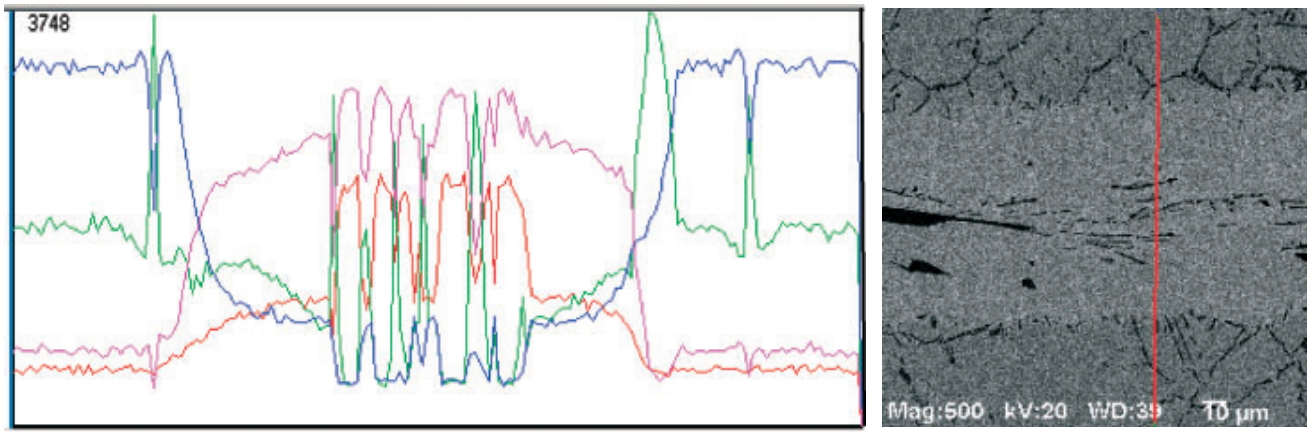

Note exclusive association of chromium with boron (not visible) and nickel with silicon

Figure 9 – Elemental distribution in a thick part of the plate/plate joint

3.2 Fecralloy/ MBF-50/ Fecralloy joints

The major characteristic of this joint is a small difference in thickness of the BM and FM. This led to involvement of the total BM cross-section in the brazing process. Figure 10 shows the BM external surface of the site opposite to the joint. The interaction with FM is particularly strong in the area opposite to the fillets where the liquid FM volume is thicker than the BM itself. Therefore, a large part of the BM, up to 80 %, was practically dissolved. A few separate seldom observed chromium borides are clearly observed and identified by EDXA at the surface (Figure 10). The general appearance of the joint cross-section is shown in Figure 11, whereas Figure 12 gives a partial view of the fillet area at high magnification. This structure is remarkably different from that of 304LN/ MBF-51 joint. First of all, the joint contains the eutectic even in the narrowest joint segment [Figures 11 a) and 11 c)]. Chromium borides have segregated as large, separate elongated faceted crystals [Figure11 b)], and as small, more or less round-shaped particles. The latter formed a very regular “chain” segregated within the braze in close proximity to the joint interface. No “decoration” of BM grain boundaries by borides is seen even in the interface zone. The dissolution of BM is very intense and uneven, resulting in the formation of a “wavy” interface [Figure 11 c) and Figure 13]. In some locations the liquid succeeded to

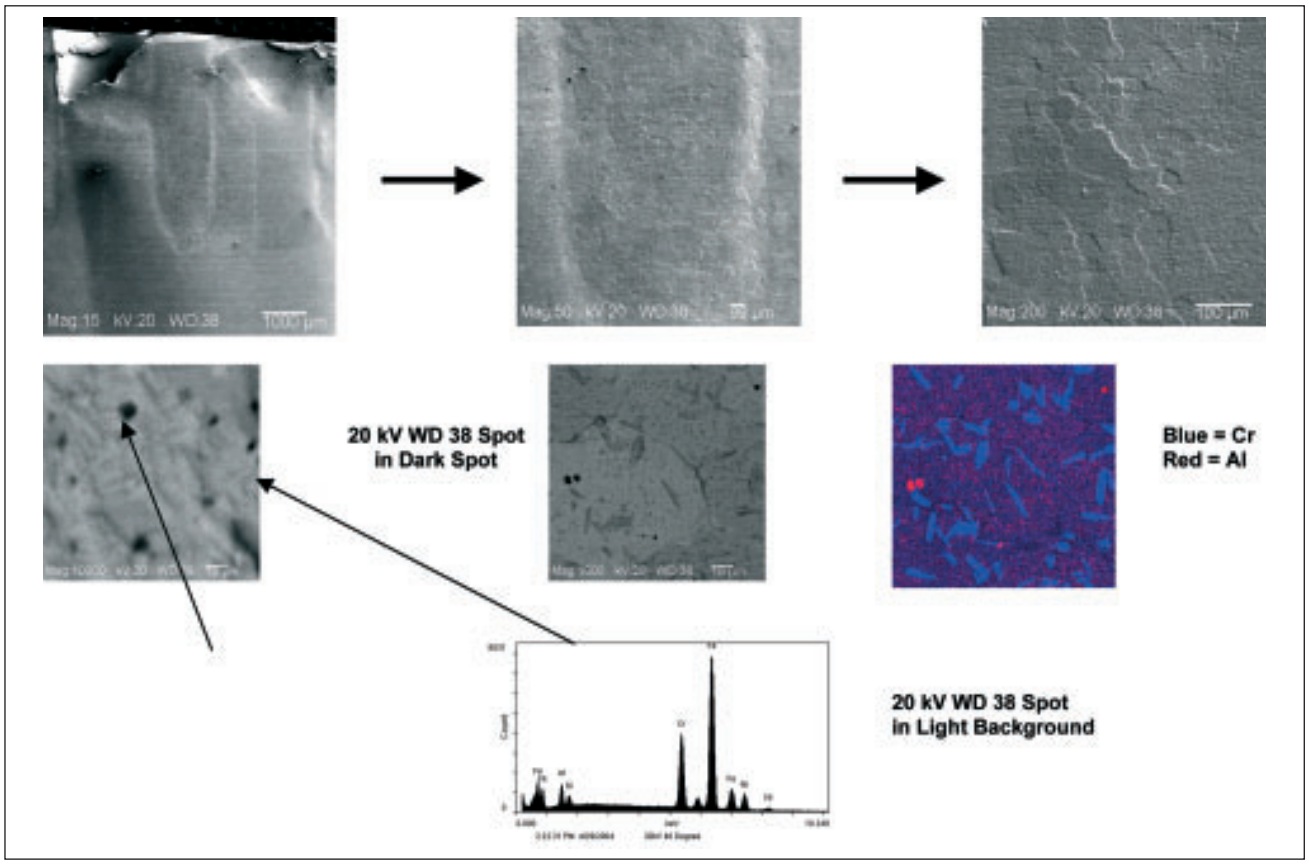

Solid arrows show magnification increase of the pictures made from the same area

Figure 10 – Outer surface of the smooth fun of the Fecralloy MBF-50 joint

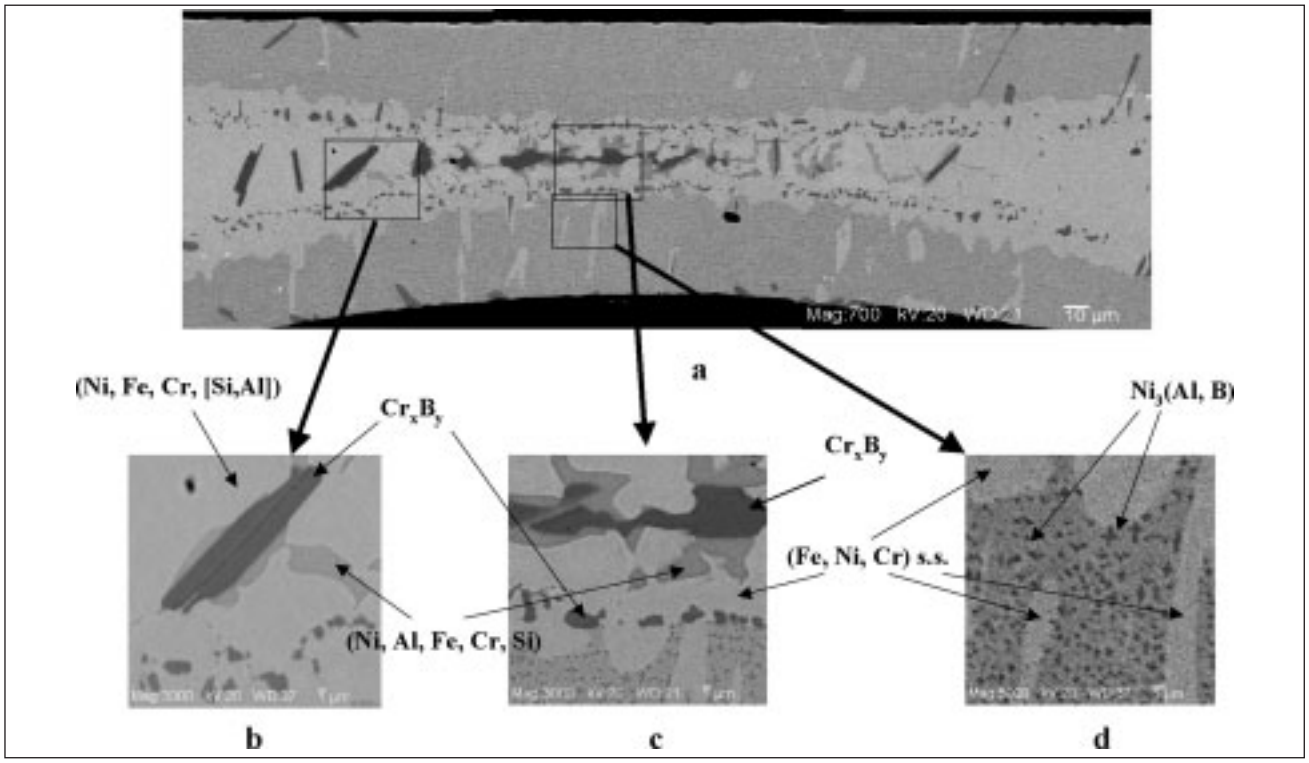

Figure 11 – Fecralloy/MBF-50 joint

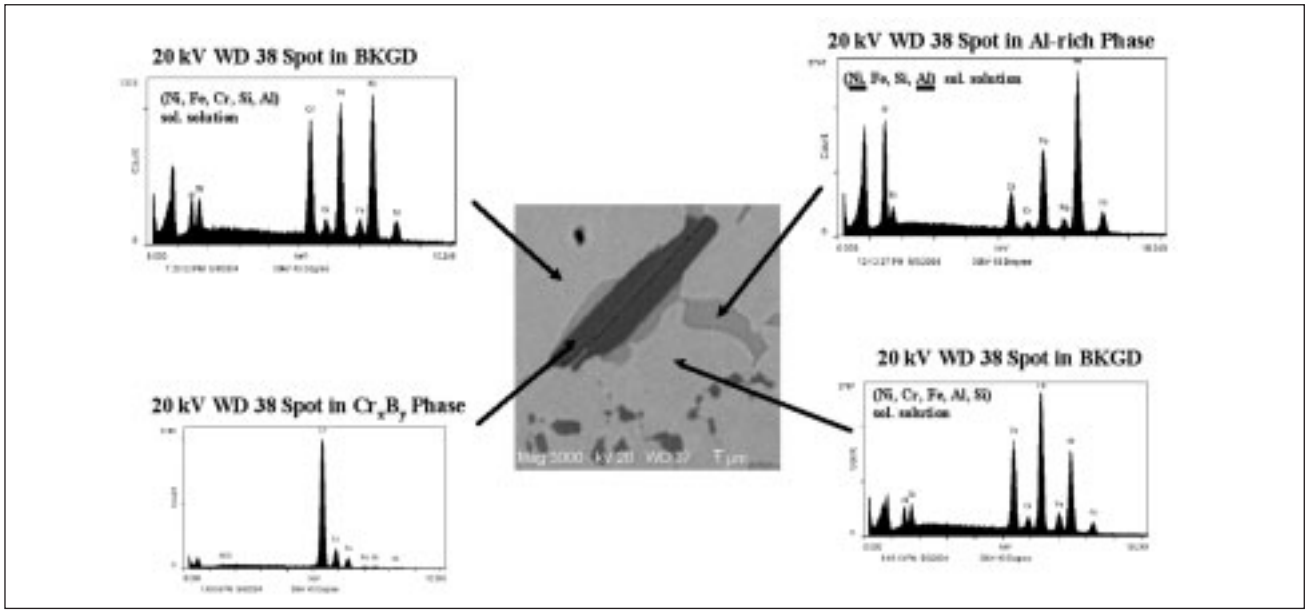

Figure 12 – Eutectic region in Fecralloy/MBF-50 joint

penetrate, dissolve BM and to form narrow channels all way to the external surface [Figures 11 a) and 11 d)]. The metallurgical reaction involved the separation of chromium together with boron, accompanied by formation of the chromium boride intermetallic crystals. At the same time, parts of nickel, chromium, silicon, and iron diffused from the BM, forming a solid solution matrix phase of the eutectic that encompasses the entire braze cross-section. Still, some of nickel and most of silicon crystallized in low-melting areas attached to large Cr_xB_y crystals which were formed first as the prime eutectic component with the highest melting temperature (Figure 12). No well-faceted intermetallic silicide crystals were observed.

The most remarkable microstructural feature of Fecralloy joints discovered here is small "sub-micron-sized" Ni_xAl_y cuboidal precipitates formed in all BM volume that was in contact with MBF-50 [Figure 11 c)]. Figure 14 shows elemental x-ray maps, which verify that these particles consist only of nickel and aluminum. These particles formed arrays, rows that are more or less parallel to the profile of the joint interface. Their formation is a result of the diffusion of nickel atoms from FM that was accompanied by simultaneous reaction of nickel with aluminum from the BM (Fe, Cr, Al) β-solid solution phase. This reaction should yield most probably an intermetallic compound having NiAl or Ni_3Al formula. Only these compounds can be formed at 1 150 °C, i.e., close

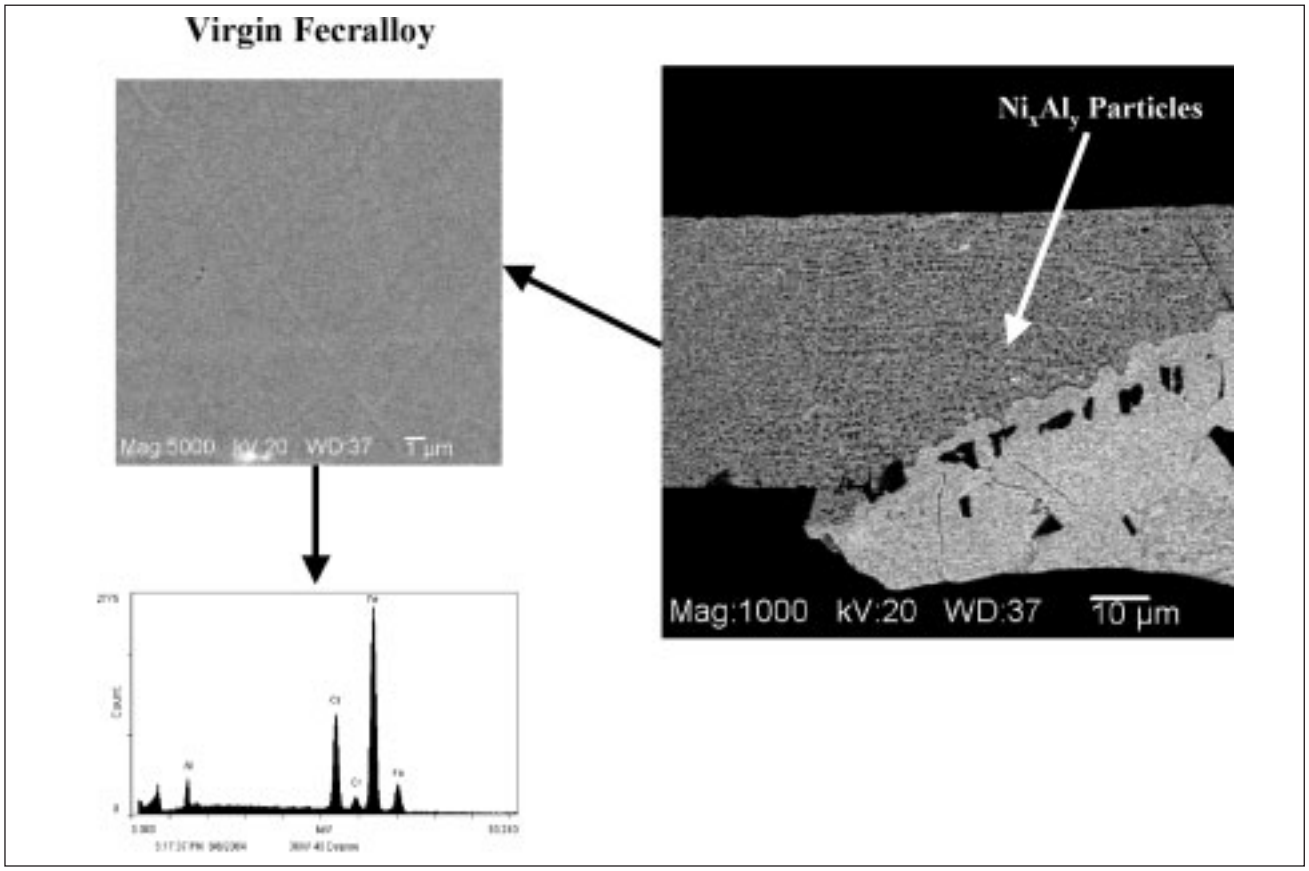

Note that Ni_xAl_y precipitations occupy BM area adjoining the interface and disappear completely at 50-60 µm distance

Figure 13 – Fecralloy/MBF-50 joint fillet area

to brazing temperature, according to two Al-Ni-Fe and Al-Ni-Cr ternary paternal phase diagrams [8]. Both components have large enthalpy of formation, –28.3 and –36.6 kcal/mole, respectively [9]. The size of particles follows nickel distribution in its diffusion profile: the larger particles are in close proximity to the interface and vice versa. Remarkably, some of these large particles have a cross-like shape [Figure 11 d) and Figure 14]. One can only speculate using the general theory of diffusion precipitation process that this cross-like shape is a way to accommodate the stress fields appearing during segregation and growth of Ni_x Al_y cuboidal particles in the matrix phase.

In general, this microstructure is similar to a typical superalloy structure of the γ' precipitation-hardened alloys with one principal distinction: here the matrix has b.c.c. crystal structure. Whereas the vast majority of the superalloys have f.c.c. Ni/Co-matrix phase in which γ-Ni_3Al cuboidal precipitates segregate providing long-term high temperature material strength. Unfortunately, neither the composition nor the crystal structure of observed Ni_x Al_y particles have so far been determined. The work in this respect is still in progress.

4 DISCUSSION

There are some important factors about the two BMs considered that result in differences in the joint microstructures. In spite of the fact that both have more or less the same chromium concentration, 304LN has γ-Fe f.c.c. crystal structure because of the presence of nickel, which places all the 300-series steels into the austenitic class. Boron has a very low solubility in the close-packed γ-phase lattice. When boron diffuses into an austenitic stainless steel BMs during brazing, it segregates at the BM grain boundaries. It is believed that "unlike many other segregants it does not cause grain boundary embrittlement in steel" [7]. There is no intragranular precipitation of Cr_xB_y crystals at relatively low boron concentrations, which is clearly seen from the results of this and other works.

Fecralloy, a ferritic-class alloy, is based on Fe-Cr-solid solution in which aluminum at 5 wt. % is completely dissolved in the solid state [10] without affecting its single-phase structure. This phase has the b.c.c. α-Fe lattice. The b.c.c. α-phase is less densely packed than γ-phase. The diffusion rate of boron atoms in α-phase is higher than in the austenitic stainless steels [11]. The presence of aluminum with a much larger atomic radius than Fe, Ni, and Cr makes the Fecralloy lattice less dense. Therefore, the α-phase can more easily accommodate chromium boride crystals when they precipitate within the grains. It also makes the α-phase receptive to fast intergranular boron diffusion. These specific circumstances seem to determine the formation of chromium borides as separate crystals, very often within BM grains.

It is worth emphasizing the importance of Ni_xAl_y precipitation for Fecralloy /MBF-50 joint performance. In spite

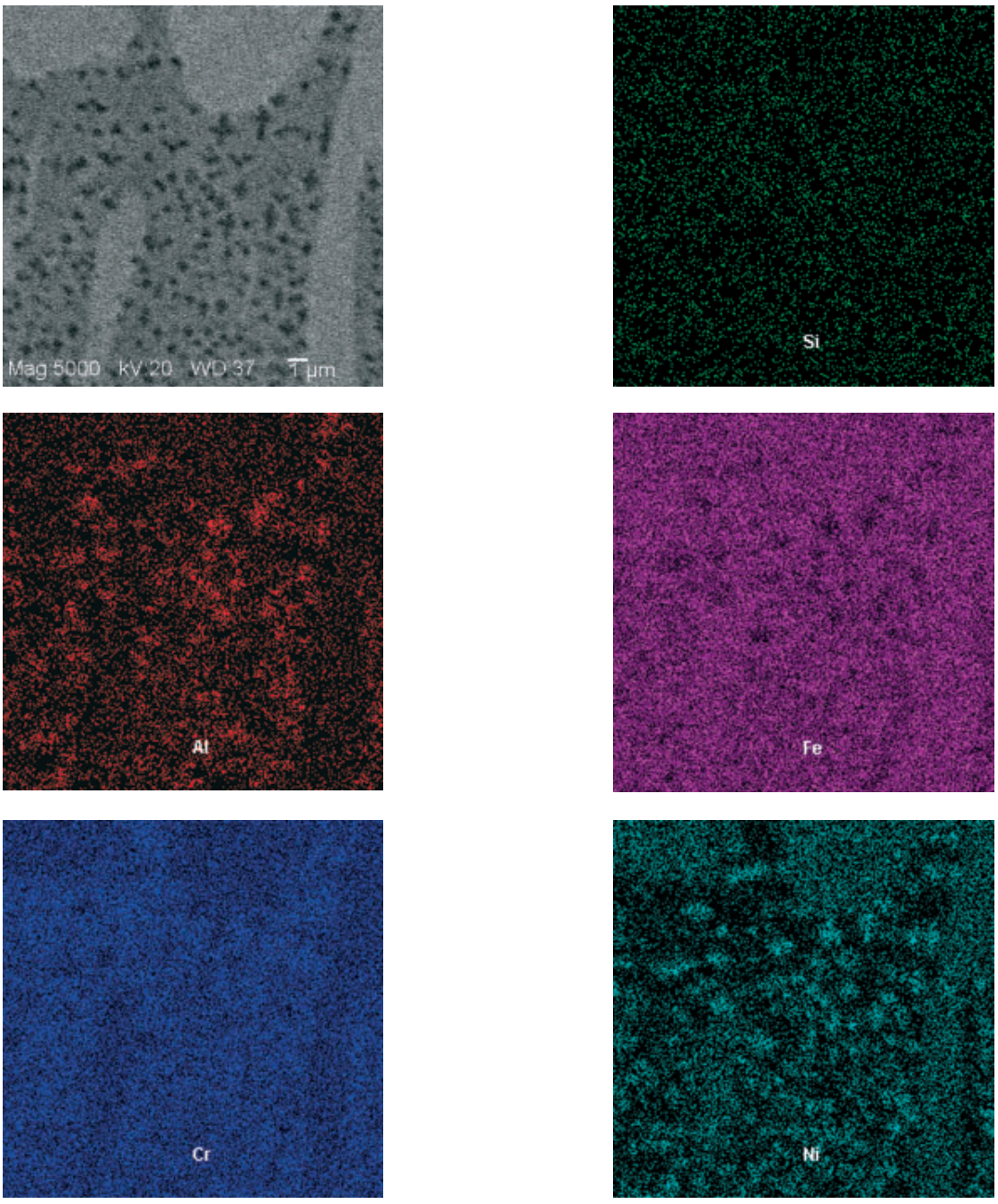

Figure 14 – SEM micrograph and x-ray elemental maps of the interface area of Fecralloy/MBF-50 joint

of the very extensive erosion of BM, the newly formed brazements become, in fact, a strong precipitation-hardened material. Preliminary shear tests of MCS samples shown in Figure 1 were prepared. The failure occurred across the cylindrical surface that encompassed 50 small joints each having a 6 mm^2 cross-section. The load-to-failure was > 3 000 kg. This load is much higher than any load, which these parts need to withstand during service. Their oxidation and corrosion resistance is also very good. This provides literally decades of reliable service lifetimes existing under the harsh conditions found in automotive exhaust pipes. Finally, Table 2 provides a compendium of the microstructural features of both joints, which readily compares their common and individual traits.

Summarizing these observations one can say that, in general, both joints have very good integrity, excellent interfaces between BM parts and brazes in all contact areas, and a favorable microstructure of the braze-core segments. No substantial porosity is observed in any part of the joints other than a few seldom and unsubstantial pores. The major point to be aware of when using these combinations of BM and FM alloys in other applications, is the possible formation of brittle chromium borides segregated in the BM parts. Our previous experience showed that in the stainless steel 316L joints brazed with MBF-51 FM, failure of the brazement occurred in the BM area adjoining the fillets, and not in the brazed area [1]. Also, large fillets usually have large chromium boride crystals that can provide crack initiation sites. Such fillets should be avoided by optimizing the part geometry. Therefore, it is very important to design the plate and fin profiles in such a way that formation of large joint areas, and particularly large fillet areas greater

Table 2 – Features of 304LN and Fecralloy joints brazed with Ni-Cr-B-Si MBF-51, -50 amorphous foils

Joint Features	304LN/ MBF-51/304LN	Fecralloy/ MBF-50/ Fecralloy
General appearance	Excellent wetting; no porosity	Excellent wetting; no porosity; wide, mostly solid solution core of the joint; no formation of Cr_xB_y at the base metal grain boundaries
Joint Phases	*Middle of Joint (d ≈ 50-100 μm):* Single γ- (Ni, Fe, Cr, Si) sol. solution phase *Close to Fillets and Fillets (d >100 μm):* Separate Cr_xB_y in γ-phase; then eutectic mixture of γ-phase, Cr_xB_y, and (Ni, Si)-solid solution; no silicides	*Middle of Joint (d ≈ 25 μm):* γ- (Ni, Fe, Cr, Si) + Cr_xB_y + (Ni,Al,Si)-phase-eutectic even within 25 μm. *Close to Fillets and Fillets (d >100 μm):* A few separate Cr_xB_y appear in γ-phase, + eutectic mixture (No silicides); More favorable fillets
Phase Morphology	Cr_xB_y plates, rods, "fans", (Ni, Si) solidified regions	Cr_xB_y plates, "fans" and rods up to 200 μm; (Ni, Al, Si) solidified solid solution
Interface/Base Metal Dissolution	Sharp interface, more or less even dissolution along complete joint cross -section indicating slow dissolution rate	Strongly eroded interface, pierced by liquid phase and needles of Cr_xB_y; Stable base metal boundaries; Chain of small Cr_xB_y crystals within the braze outlining interface.
Base Metal	Three affected morphological zones adjoining interface in the following order: 1. Small grains similar to perlite formed by f.c.c. γ-phase sol. solut. + Cr_xB_y (5-10 μm) 2. Large virgin grains completely outlined by Cr_xB_y, segregated sometimes also at twin boundaries (30-40 μm) 3. Large virgin grains partially outlined by narrow Cr_xB_y crystals (> 40 μm)	Fine $Ni_3(Al,B)$ precipitates segregate intergranularly across complete base metal within (Fe,Cr,Al) solid solution providing strong precipitation hardening of corrosion and oxidation resistant matrix. Chromium borides segregate intergranulary without affecting base metal grain boundaries.

than 150 μm will be avoided. Moreover, it is strongly recommended to have brazing gap widths not exceeding 50-70 μm. It was also shown that post-brazing annealing of 300 stainless steel/MBF brazements might substantially improve the ductility, and the maximum stress-to-failure values [1]. Such secondary treatment is worth considering for these joints in the future.

5 SUMMARY

1. Vastly different microstructures are formed in brazed joints 304LN/ Ni-15Cr-1.4B-7.25Si (MBF-51) and Fecralloy®/Ni-19Cr-1.5B-7.3Si (MBF-50). Detailed descriptions are given for the composition and morphology of phases evolved in these brazements, which results from complex metallurgical reactions between base and filler metals.

2. A new metallurgical reaction was discovered between b.c.c. Fe-20Cr-5Al BM and Ni and B diffused from Ni-19Cr-1.5B-7.25Si. This reaction results in precipitation of fine, regularly distributed $Ni_x(Al)_y$ particles in the BM matrix phase, thus strengthening Fecralloy brazements.

3. The microstructure discovered in this work is remarkably similar to conventional precipitation-hardening alloy microstructures. This explains why Fecralloy/MBF-50 joints can withstand years of service in the brutal environment of automotive exhaust pipes.

ACKNOWLEDGEMENTS

We are very thankful to Mr. Steve Ayres (Garret Division, Honeywell) for cooperation and providing samples, and permission to publish our data.

REFERENCES

[1] Rabinkin A., Wenski E., Ribaudo A.: Brazing stainless steel using a new MBF- series of Ni-Cr-B-Si amorphous foil, Weld. J., 1998, 77, No. 2, pp. 66s-75s.

[2] Rabinkin A.: Optimization of brazing technology, structural integrity, and performance of multi- channeled, three dimensional metallic structures, Proceedings of the International Brazing and Soldering Conference, 2000, pp. 437-444, Albuquerque.

[3] Rabinkin A.: Overview: Brazing with (NiCoCr)-B-Si amorphous brazing FMs: Alloys, processing, joint structure, properties, applications, Sci. Tech. Welding and Joining, 2004, 9, No. 3, pp. 181-199.

[4] Rabinkin A.: Brazing with amorphous foil preforms, Adv. Mat. Proc., 2001, 159, No. 6, pp. 65-67.

[5] Heikinheimo L., Miglietti W., Kipnis J., Leone E., Rabinkin A.: Brazing of Co- and Ni- based superalloys using new amorphous brazing filler metals, in LOT01, DVS, Aahen, 2001, pp. 468-475.

[6] Karlson L., Norden H.: Non-equilibrium grain boundary segregation of boron in austenitic stainless steel – IV. Precipitation Behavior and distribution of elements at grain boundaries, Acta Metal., 1988, 36, No. 1, pp. 35-48.

[7] Karlson L., Norden H., Odelius H.: Non-equilibrium grain boundary segregation of boron in austenitic stainless steel – I. Large Scale segregation behavior, Acta Metal., 1988, 36, No. 1, pp. 1-12.

[8] Villars P., Prince A., Okamoto H.: Handbook of Ternary alloy phase diagrams, ASM, 3, 1995, p. 3156 and p. 3538.

[9] Kubaschewski O., Alcock C.B.: Metallurgical thermochemistry, Univ. Toronto, 5th Ed., 1978, pp. 300-301.

[10] Villars P., Prince A., Okamoto H.: Handbook of Ternary alloy phase diagrams, ASM, 3, 1995, pp. 3105-3118.

[11] Wang W., Zhang S., He X.: Diffusion of boron in alloys, Acta Metal. & Mat., 1995, 43, pp. 1693-1699.